Supplement of Solid Earth, 15, 1029–1046, 2024
https://doi.org/10.5194/se-15-1029-2024-supplement

Solid Earth Open Access EGU

Supplement of

Post-Caledonian tectonic evolution of the Precambrian and Paleozoic platform boundary zone offshore Poland based on the new and vintage multi-channel reflection seismic data

Quang Nguyen et al.

Correspondence to: Quang Nguyen (qnguyen@igf.edu.pl)

Supplementary material

Supplementary text

Multiple reflection elimination strategies

Multiple reflection (multiples) are a constant problem for marine seismic data and even a more challenging issue in shallow waters. The water depth of the southern Baltic Sea is mostly from 10 to 50 m. Therefore, the seismic records in this area will be always contaminated with multiple reflections, especially at near seafloor intervals.

The application of multiple reflection removal (demultiple) methods is dependent on the properties of the multiple present in the seismic data (Verschuur, 2013). There are two main categories: (1) methods based on a difference in spatial behaviour of primaries and multiples; and (2) methods based on periodicity and predictability. The former is typically based on filtering methods such as τ-p deconvolution, Radon demultiple or stacking, which exploits the differences in velocities and/or reflecting structures between the primaries and multiples. The latter relies on the prediction from either modelling or inversion of the recorded seismic wavefield (Weglein, 1999). Surface-related multiple elimination (SRME) or wavefield extrapolation methods are among this category (Verschuur, 2013).

Multiple reflection elimination strategies applied to BalTec profiles

SRME is a method using a data-driven algorithm for removing multiples (Verschuur et al., 1992) that is often applied earlier than other demultiple approaches in the processing flow. However, SRME's efficiency is largely affected by the signal-to-noise ratio of the input data. Therefore, gun and cable static correction, spherical divergence, and other incoherent noise attenuation approaches should be applied to the SRME input while maintaining the amplitudes and phase of recorded primaries and multiples. The shot point interval is 25 m while the channel interval is 12.5 m. Therefore, to construct the multiple estimates, the shot points were interpolated to 12.5 m, and the record data are extrapolated to zero offsets. A mute is applied to the input shot records prior to removing direct arrival energy and the first seafloor multiple. After surface-related multiple is modelled by a series of convolutions and summation, the output model shot point is renumbered back to the same order as the original shot gathers for the subtracting process. For this data, a three-passes approach for SRME adaptive subtraction including two subtraction processors based on two publications by Wang (2003) and Monk (1993) is applied.

The τ-p predictive deconvolution method is applied following the SRME method. The main aim of τ-p deconvolution for this dataset is to remove short-path multiples. At the same time, muting performed in the τ-p domain attenuates linear noise and

seismic interference. The input data is transformed to the τ-p domain using linear transform (Stoffa et al., 1981; Zhou and Greenhalgh, 1994), Wiener deconvolution (design window of 240 ms of operator length and 48 ms of gap length) is applied to the whole traces. After τ-p deconvolution, in order to improve signal-to-noise ratio and enhance deeper imaging data were regularized in 2 steps. Firstly, the shot records are interpolated to 12.5 m of shot point interval from the nominal 25 m recorded, which doubled the CDP fold. Secondly, decimating the fold of the shot gathers from 216 to 113 to get to a 25 m receiver interval and 12.5 m CDP interval so the spatial sampling at 12.5 m is more beneficial to image the deeper part of the sections.

Because of the very shallow water bottom, SRME does not successfully eliminate strong water bottom multiples. Therefore, to remove them, we used a simple technique in which the data are flattened according to the travel time of the water-bottom multiple followed by a F-K reject mute to remove flattened multiple energy (see Nguyen, 2020). This procedure (called the water bottom F-K filtering approach) can be repeated for the N-th water bottom multiple. Here, we applied up to three passes.

Parabolic Radon demultiple (PRT demultiple) is applied to target the long-path multiples as SRME and τ-p predictive deconvolution methods are inefficient for these types of noises. The normal PRT demultiple has some limitations, so a Harlan signal extraction filter (based on Harlan, 1995) is used to overcome the limitations (this approach was called high-resolution PRT demultiple). This filter provides a high-resolution Radon transform by taking the PRT of the input data, and the muted PRT of the input data with trace polarities randomly reversed and put these into Harlan's signal extraction algorithm to focus on the signal in the PRT domain. The high-resolution PRT demultiple is applied with a start time of 500 ms as artefacts are introduced in the near-surface, where move-out values are large and reflections only exist at near offsets. Optionally, this approach also is reapplied after each velocity analysis pass.

Evaluation of the effectiveness of the demultiple strategies applied to BalTec profiles

Seismic gathers in the shot and CDP domain after each demultiple method are compared in Figure S1. A series of stack sections after each demultiple approach are shown in Figure S2. The first demultiple approach used in the processing flow is SRME to suppress the dominant short-path multiples in the shot domain (red arrows in Fig. S1a). These multiples may represent peg-legs which bounce once or more between the seafloor and the high amplitude reflecting plane below (potentially the top Silurian) (Levin and Shah, 1977), and reverberations of the seafloor and strong reflection events (McGee, 1991). Given that the SRME was more effective in the deeper part of the shot gather, it was chosen over the predictive deconvolution in this case. The shot gather after SRME shows short-path multiples and surface-related multiples successfully suppressed (Fig. S1b), especially at near-offset due to the sensitivity of the SRME algorithm in near-offset multiple reconstructions (Qu et al., 2021).

The τ-p deconvolution when performed together with muting in the τ-p domain addressed different types of noise besides multiples, i.e. direct wave, seismic interference, or guided waves (Fig. S1b). The direct waves travel directly from sources to

receivers and appear as linear event in the gather (black arrows in Fig. S1b), they are a typical type of noise in any marine seismic dataset. Whereas the guided waves are commonly found in seismic data from shallow water environments and are most recognized in far offset in the field record (green arrows in Fig. S1b) (Yilmaz, 2001). The guided waves in the shot gather probably represent multiples of the refracted energy. The example of a shot gather after applying τ-p deconvolution (Fig. S1c) and τ-p mute shows a much cleaner gather without these linear coherent noises, and increases the primary event at far offset. The seismic interference (blue arrows in Fig. S1b) was also suppressed by τ-p deconvolution, this type of noise usually happens during a multi-vessel acquisition. In this case, the seismic interference and primary events could be separated in the τ-p transform domain because of their contradicting dips (Gulunay et al., 2004; Elboth et al., 2017).

The example stack sections from line BGR16-202 display a great improvement after the demultiple workflow (Fig. S2). There is noticeable suppression of noise and multiples (black arrows in Fig. S2a). Furthermore, primary events are enhanced to avoid misinterpretation (examples in the oval areas in Fig. S2b). However, the first and second order of the water bottom multiples still exist in the BalTec data stack section (black arrows in Fig. S1c) because it is difficult to predict these events using the SRME algorithm owing to insufficient number of traces in this very shallow water depth area. Therefore, the water bottom F-K filtering approach was applied in the shot domain to eliminate these shallow water bottom multiples. The stack section after this method (Fig. S2d) shows that the dipping primary reflections are no longer interfered with by multiples associated with the water bottom.

The methods based on velocity discrimination might not work properly for the multiples that appeared in the shallow part of the pre-stack gathers since the move-out difference is not big enough, and the number of traces or samples which are not muted by NMO stretch mute is too sparse. Therefore, the high-resolution PRT approach targets the multiples in the deeper part of the CDP gathers (yellow arrows in Fig. S1d) that have larger move-out compared to the primary reflections due to much longer travel path (Hampson, 1986; Sacchi and Ulrych, 1995). The high-resolution PRT approach provided very promising results (Fig. S1e) in cleaning the CDP gather where the NMO-corrected primary events were no longer distracted by large move-out multiples, making velocity picking on such gathers much easier. However, when the data are stacked, there are not that many differences between the data with/without the Radon demultiple applied. Removal of these long-path multiples also helps to increase signal-to-noise ratios by later stacking process.

Velocity analysis and migration of BalTec profiles

The velocity models were determined using the interactive velocity analysis program (Global Claritas CVA). Generally, velocity analysis was carried out in 3 passes: the first pass velocity is picked before the high-resolution Radon demultiple, the second pass is picked and updated before pre-stack time migration, and the third pass is checked and updated the second pass

velocity after migration. Velocity was picked at every 500 CDP point for the first pass, then 250 CDPs (around 3.0 km intervals) for the next two passes. A straight-ray 2D Kirchhoff pre-stack time migration (PSTM) is performed using first-pass velocities to enhance data imaging. The main input of the migration process is pre-stack seismic data with geometry applied and picked RMS velocity field. The pre-stack migration process is applied again when each pass of the velocity field is updated. Before stacking, a post-NMO outer trace mute is applied to remove any coherent noise on the outer traces and to reduce the effect of NMO stretching on the far offsets. To balance seismic amplitude across the section, a normal 500 ms window AGC scaling process is applied before and after stacking.

Reprocessing of the legacy PGI97 data

In case of the PGI97 data, other than the usual linear events that were handled by the F-K filter, the main types of multiples existing in the shot gathers were short-path reverberations and water bottom multiples (Fig. S3b and c). The limited offset of the PGI97 data (~140 m streamer length and 12 channels) constrains the application of modern demultiple approaches. Therefore, simple predictive deconvolution (24 ms gap and 300 ms operator length) in the X-T domain is applied to suppress the reverberations. The shot gathers after the predictive deconvolution approach shows noticeable multiples removed, represented by much cleaner autocorrelation functions (AC in Fig. S3c). The water bottom F-K filtering method proves the efficiency by eliminating first and second-order multiples generated by the water bottom (Fig. S3d).

References

Elboth, T., Shen, H., and Khan, J.: Advances in Seismic Interference Noise Attenuation. Presented at the 79th EAGE Conference and Exhibition 2017, European Association of Geoscientists & Engineers, 1–5, https://doi.org/10.3997/2214-4609.201700579, 2017.

Gülünay, N., Magesan, M., and Baldock, S.: Seismic Interference Noise Attenuation. Paper no. SEG-2004-1973, presented at the 2004 SEG Annual Meeting, OnePetro, Denver, Colorado, October, 2004.

Hampson, D.: Inverse velocity stacking for multiple elimination, in: SEG Technical Program Expanded Abstracts 1986, SEG Technical Program Expanded Abstracts. Society of Exploration Geophysicists, 422–424, https://doi.org/10.1190/1.1893060, 1986.

Harlan, W.S.: Regularization by model reparameterization, http://www.billharlan.com/papers/regularization.pdf, 1995.

Levin, F.K., and Shah, P.M.: Peg-leg multiples and dipping reflectors. Geophysics, 42, 957–981, https://doi.org/10.1190/1.1440775, 1977.

McGee, T.M.: Seismic reverberations and the remote estimation of properties of underwater soils. Int. J. Imaging Syst. Technol., 3, 40–57, https://doi.org/10.1002/ima.1850030107, 1991.

Monk, D.J.: Wave-equation multiple suppression using constrained gross-equalization. Geophys. Prospect., 41, 725–736, https://doi.org/10.1111/j.1365-2478.1993.tb00880.x, 1993.

Nguyen, Q.: Seismic Data Processing Report (BALTEC / MSM52). Institute of Geophysics PAS, https://dspace.igf.edu.pl/xmlui/handle/123456789/112 (last access: 25/04/2024), 2020.

Qu, S., Verschuur, E., Zhang, D., and Chen, Y.: Training deep networks with only synthetic data: Deep-learning-based near-offset reconstruction for (closed-loop) surface-related multiple estimation on shallow-water field data. Geophysics, 86, A39–A43, https://doi.org/10.1190/geo2020-0723.1, 2021.

Sacchi, M.D., and Ulrych, T.J.: High-resolution velocity gathers and offset space reconstruction. Geophysics, 60, 1169–1177, https://doi.org/10.1190/1.1443845, 1995.

Stoffa, P.L., Diebold, J.B., and Buhl, P.: Inversion of seismic data in the τ-p plane. Geophys. Res. Lett., 8, 869–872, https://doi.org/10.1029/GL008i008p00869, 1981.

Verschuur, D.J., Berkhout, A.J., and Wapenaar, C.P.A.: Adaptive surface-related multiple elimination. Geophysics, 57(9), 1166–1177, https://doi.org/10.1190/1.1443330, 1992.

Wang, Y.: Multiple subtraction using an expanded multichannel matching filter. Geophysics, 68, 346–354, https://doi.org/10.1190/1.1543220, 2003.

Weglein, A.B.: Multiple attenuation: an overview of recent advances and the road ahead (1999). Lead. Edge, 18, 40–44, https://doi.org/10.1190/1.1438150, 1999.

Yilmaz, Ö.: Seismic Data Analysis: Processing, Inversion, and Interpretation of Seismic Data. Society of Exploration Geophysicists, https://doi.org/10.1190/1.9781560801580, 2001.

Zhou, B., and Greenhalgh, S.A.: Linear and parabolic tau -p transforms revisited. Geophysics, 59, 1133–1149, https://doi.org/10.1190/1.1443669, 1994.

Supplementary figures

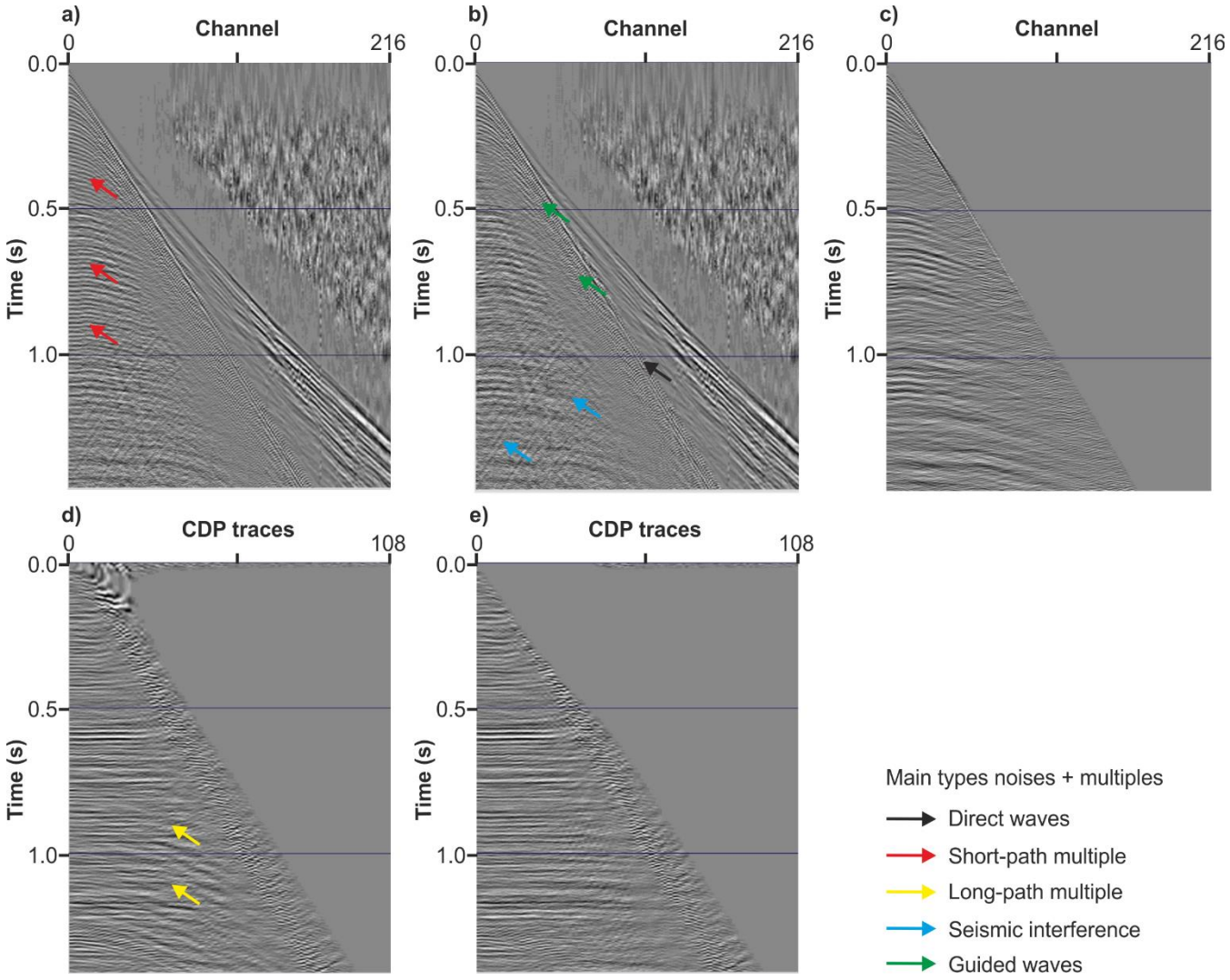

Figure S1: Example of shot gathers and CDP gathers after the main processing steps of the BalTec data. (a) Raw shot gather; (b) Shot gather after SRME; (c) Shot gather after τ-p deconvolution; (d) CDP gather after water bottom F-K filtering (input for Radon demultiple); (e) CDP gather after Radon demultiple. The main types of noises and multiples are highlighted by arrows. Notice how different events are attenuated after each demultiple approach.

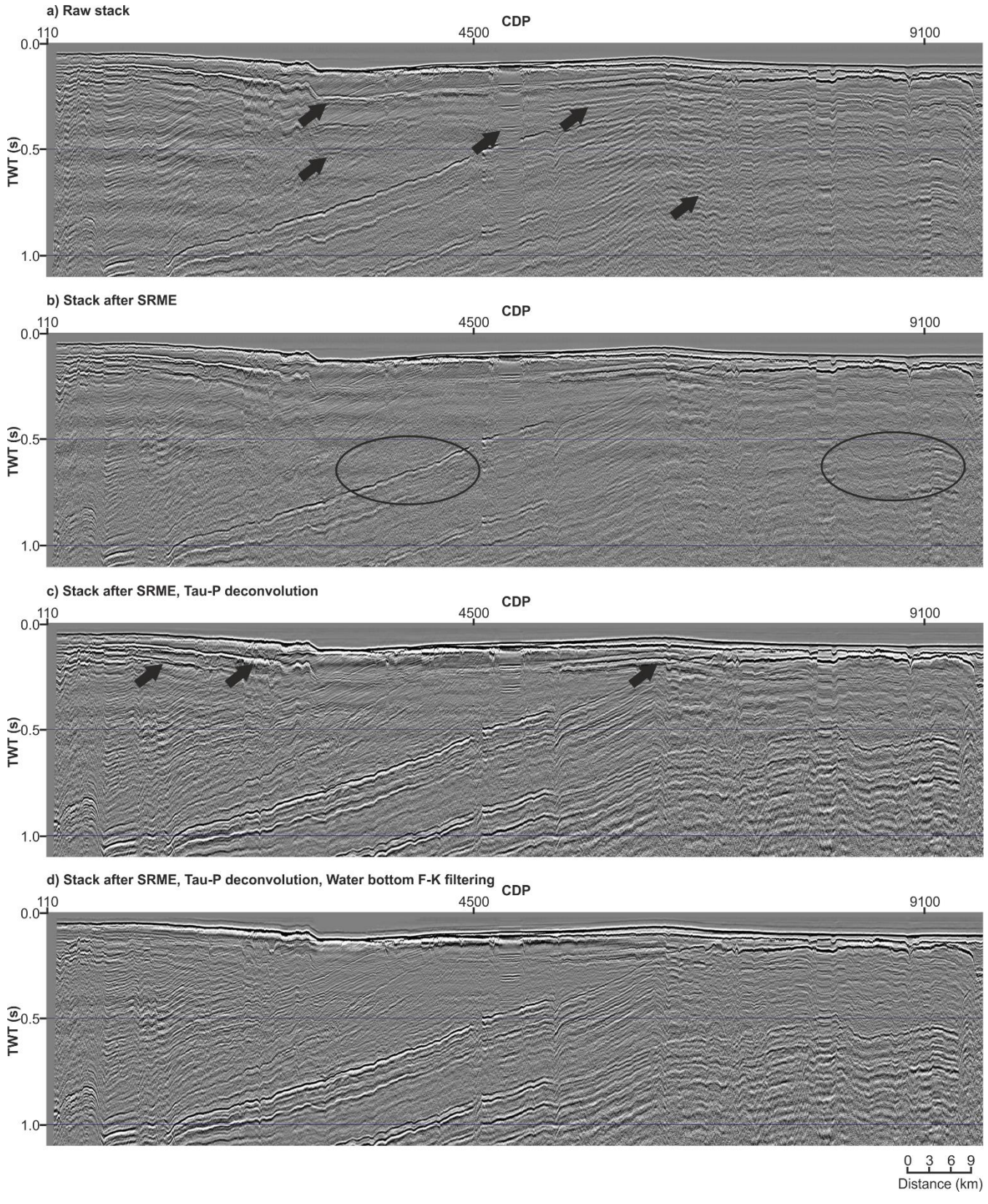
a) Raw stack
CDP
110
4500
9100
0.0
0.5
1.0
TWT (s)
b) Stack after SRME
CDP
110
4500
9100
0.0
0.5
1.0
TWT (s)
c) Stack after SRME, Tau-P deconvolution
CDP
110
4500
9100
0.0
0.5
1.0
TWT (s)
d) Stack after SRME, Tau-P deconvolution, Water bottom F-K filtering
CDP
110
4500
9100
0.0
0.5
1.0
TWT (s)
0 3 6 9
Distance (km)

Figure S2: Part of stack sections of line BGR16-202. (a) Raw stack; (b) Stack after SRME; (c) Stack after SRME and τ-p deconvolution; (d) Stack after SRME, τ-p deconvolution, and Water bottom F-K filtering. Black arrows highlight attenuated multiples after each demultiple approach. Oval areas show examples of improved reflections.

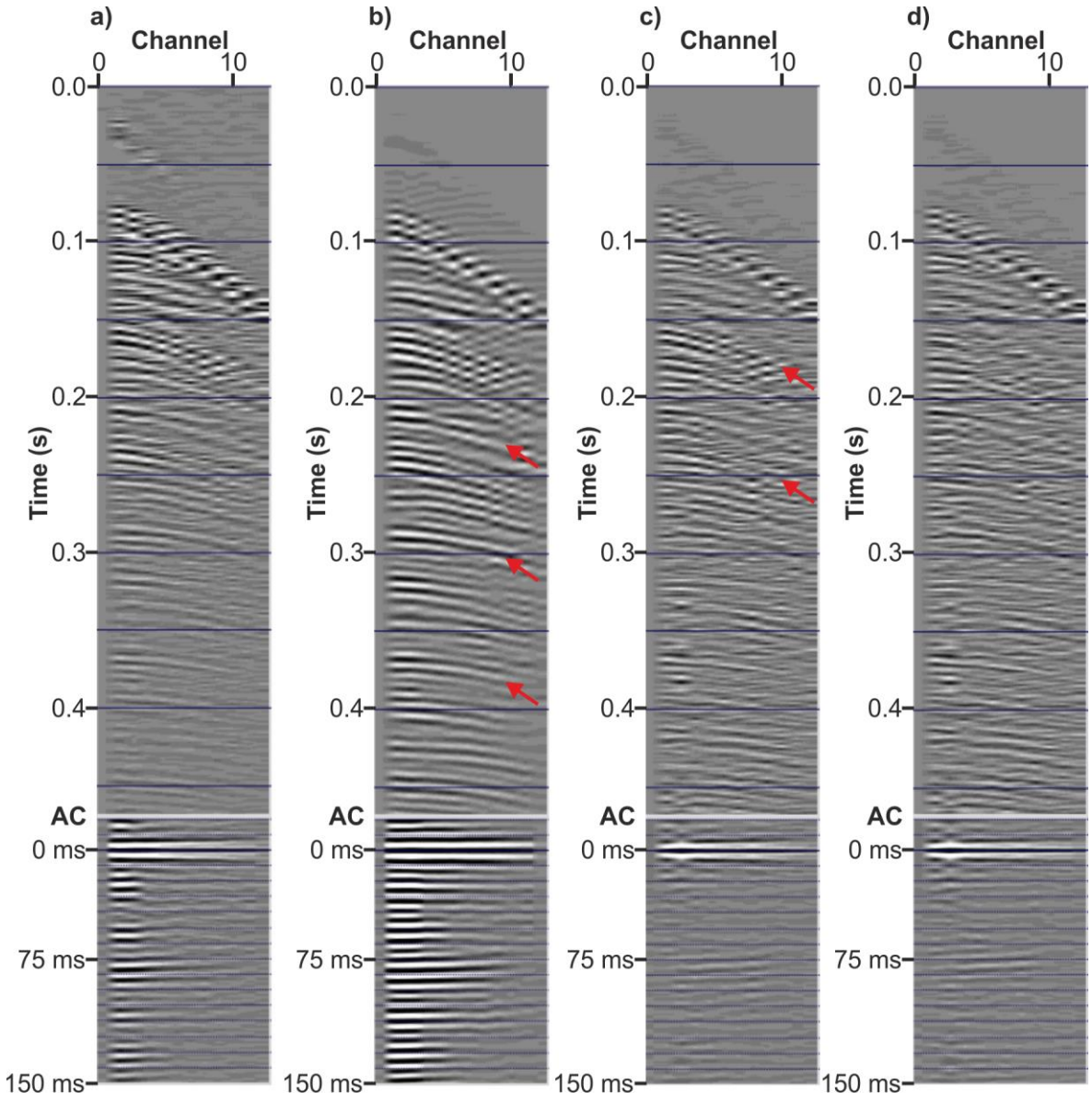

Figure S3: Example of shot gathers after main processing steps of the PGI 97 data and their autocorrelation (AC); (a) Raw shot gathers, (b) Shot gathers after FK mute and spherical divergence, (c) Shot gathers after predictive deconvolution, (d) Shot gathers after water bottom F-K filtering. Notice the visible attenuation of reverberation in the AC after the predictive deconvolution.

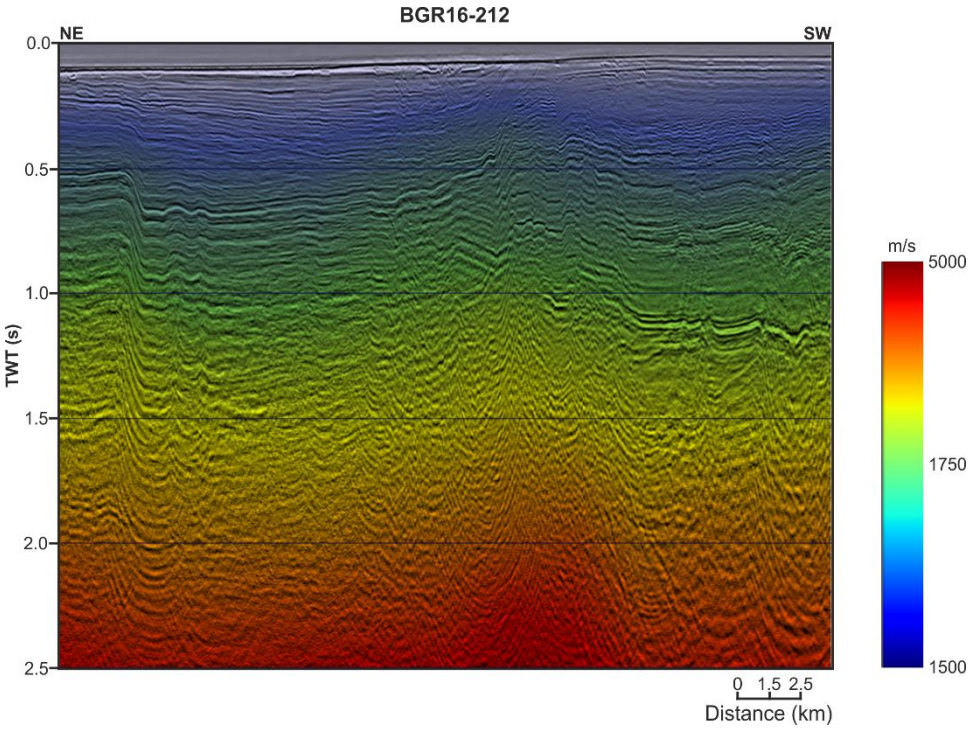

Figure S4: Part of RMS velocity model (line BGR16-212) at the Koszalin Fault zone.

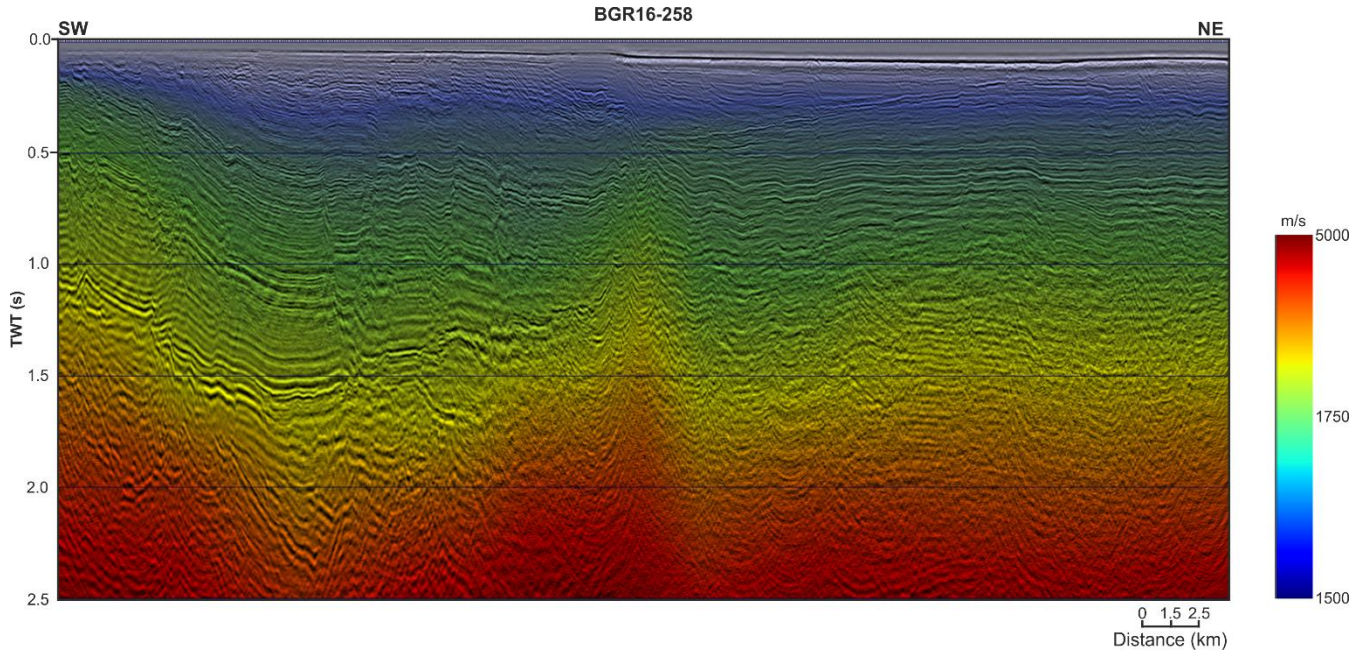

155 **Figure S5:** Part of RMS velocity model (line BGR16-256) at the Koszalin Fault zone.

a) Velocity analysis procedure

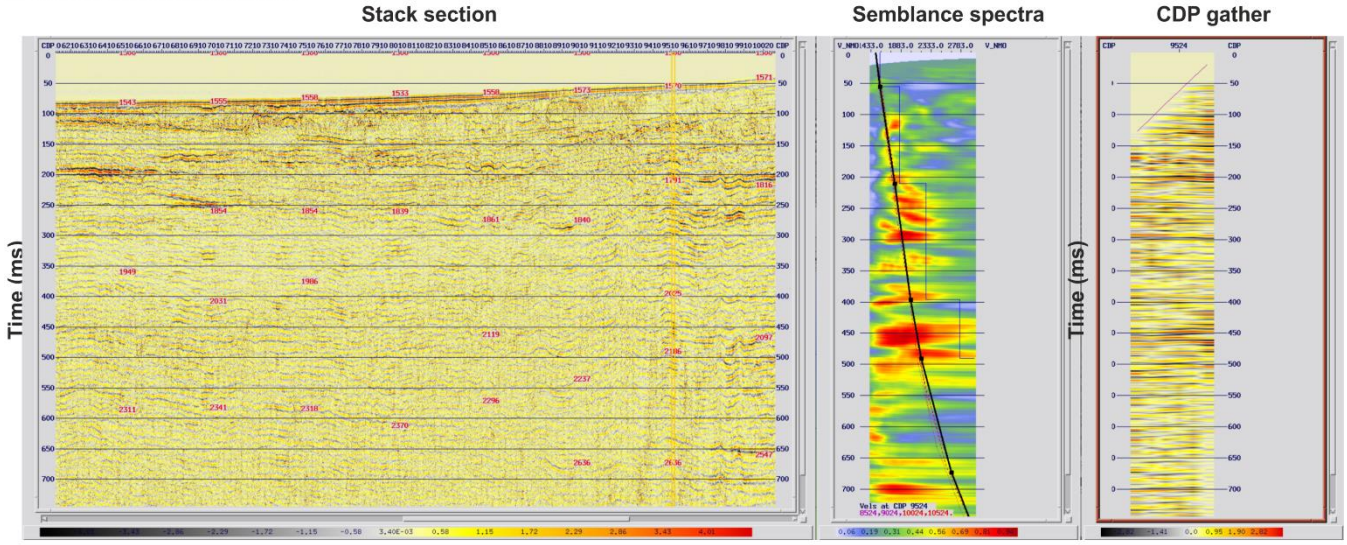

b) An example of new RMS velocity model (line PGI97-1301)

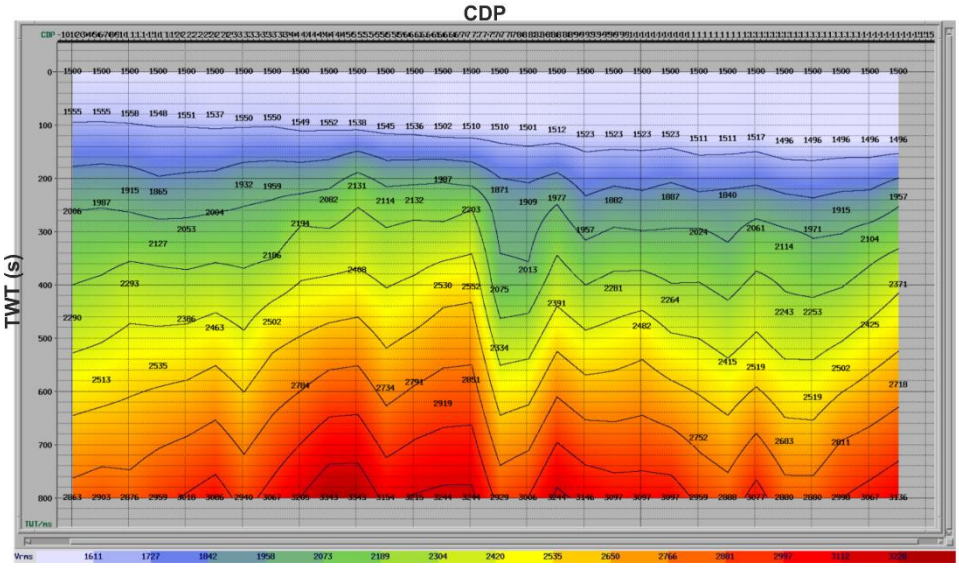

Figure S6: Velocity analysis procedure (a) and example of the velocity model (b) of the PGI97 reprocessing workflow.

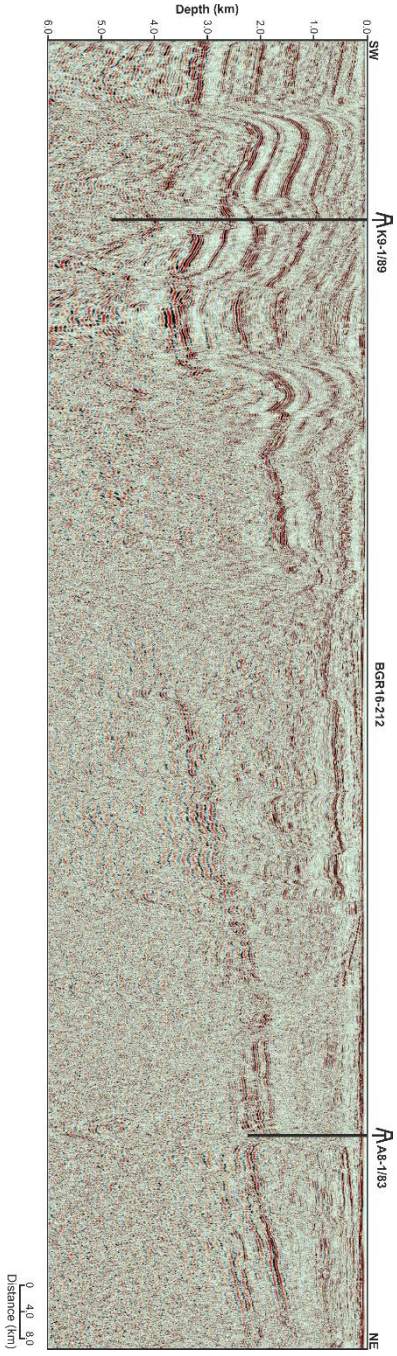

Figure S7: Example of processed line BGR16-212 in depth (see location in Fig. 1B). Depth conversion using stacking velocity (Fig. S4). For full interpretation please refer to Ponikowska et al. (2024).